PRINT ISSN 1119-8362
Electronic ISSN 2659-1499

Full-text Available Online at
https://www.ajol.info/index.php/jasem
https://www.bioline.org.br/ja

J. Appl. Sci. Environ. Manage.
Vol. 28 (10B Supplementary) 3439-3452 October, 2024

Assessment of Aquifer-Protective Capacity of Orire Estate in Akure, Ondo State, Nigeria

[1]OLATUNJI-ADENIYI, O; [2]AYUA, KJ; [3]*OSISANYA, OW

[1]Department of Applied Geophysics, Federal University Of Technology, Akure. Ondo state.
[2]Department of Physics, Federal University Lokoja, Kogi State, Nigeria
**[3]Department of Physics, Federal University of Petroleum Resources, Effurun, Delta State.*

Corresponding author Email: wasiu.osisanya@uniben.edu
**ORCID ID: https://orcid.org/0000-0001-7280-9771*
**Tel: +2347036555765*

Co-Author Email: olamidotunadeniyi@yahoo.com; ayuakj@gmail.com

ABSTRACT: The amount and thickness of clay layers and surrounding organic elements have a direct impact on how well an aquifer protects itself. Thus, the purpose of this work was to evaluate Orire Estate's ability to preserve the aquifer in Akure, Ondo State, Nigeria, using a geophysical survey that used the Vertical Electrical Sounding (VES) and Very Low Frequency (VLF) Electromagnetic Technique. Throughout the course of the survey, seven traverses of various lengths were established, and VLF-EM measurements were made every five meters along the four main profiles. Thirteen vertical electrical soundings were also performed, with electrode spacings varying from one to one hundred meters. Computer-assisted modeling and partial curve matching approaches were used in the interpretation of the data. Four subsurface geological units were identified by the analysis: topsoil, worn layer, fractured basement, and fresh basement. The topsoil layer, with a thickness ranging from 0.9 to 1.5 meters, exhibited resistivity values between 57.0 and 198.4 Ω-m. The worn layer varied in thickness from 2.6 to 17 meters, with resistivity values from 87.0 to 978.7 Ω-m. The fractured basement layer's thickness ranged from 7.8 to 23.7 meters, showing resistivity values between 311 and 3041.8 Ω-m, while the fresh basement layer demonstrated resistivity values ranging from 1423.1 to 3790.57 Ω-m with infinite thickness. The presence of zones with poor aquifer-protective capacity throughout the study area indicates a heightened vulnerability to contamination from leachates and other pollutants. The subsurface conditions suggest an abundance of unconsolidated sand with limited clay, which prolongs the residence time of percolating pollutants and diminishes the necessary impediment to fluid movement for effective filtration.

DOI: https://dx.doi.org/10.4314/jasem.v28i10.61

Cite this Article as: OLATUNJI-ADENIYI, O; AYUA, K. J; OSISANYA, O. W (2024). Assessment of Aquifer-Protective Capacity of Orire Estate in Akure, Ondo State, Nigeria. *J. Appl. Sci. Environ. Manage.* 28 (10B Supplementary) 3439-3452

Dates: Received: 21 August 2024; Revised: 29 September 2024; Accepted: 08 October 2024 Published: 31 October 2024

Keywords: Aquifer Protection; Groundwater Quality; Subsurface contaminants; Geophysical survey.

The water found beneath the earth's surface in soil, rock, and fractures in rock formations is known as groundwater. Groundwater is a valuable natural resource that holds significant economic and social importance. It accounts for over thirty percent of the world's freshwater supply, or roughly 0.76% of all water on Earth, including ocean and permanent ice. Approximately 98% of the liquid freshwater on Earth is found in groundwater, which is widely dispersed throughout the planet (Wikipedia.org/wiki/Groundwater). For home, industrial, and agricultural applications, groundwater is extremely important. Potable and safe drinking water is the only thing that a society's members need for good health and a productive existence. Nearly half of the world's drinking water comes from

**Corresponding author Email: wasiu.osisanya@uniben.edu*
**ORCID ID: https://orcid.org/0000-0001-7280-9771*
**Tel: +2347036555765*

groundwater, which also provides more than 40% of the water used globally for irrigation in agriculture (Olorunfemi and Fasuyi, 1993). In most cities and towns, it is impossible to maintain a high-quality groundwater supply free from chemical and microbiological pollution (Satpatty and Kanugo, 1976). One could have expected that adequate attention would have been paid to aquifer conservation in order to minimize groundwater quality degradation, given the significance of groundwater for drinking sources. However, aquifer preservation has not received enough attention until relatively recently, especially in and around urban and industrial regions where many real or prospective sources of contamination are located (Eyankware, 2019; Eyankware and Aleke, 2021). The rapid growth in population has resulted in issues with the availability of clean water, which poses a major risk to human health because of the careless disposal of garbage from cities, businesses, and farms. Typically, these pollutants produce leachate plumes that can affect groundwater basins. Numerous issues are causing the quality of water supplies to deteriorate on a worldwide scale. Anthropogenic activity is a major element affecting the water quality, especially in the research region. Numerous scientific disciplines, such as microbiology, biochemistry, geology, and others, have persisted in analyzing the progressive deterioration of water quality (Eyankware, *et al.,* 2023a; Opara *et al*., 2022). For accurate interpretation, a thorough understanding of the research area's hydrogeology and geology is essential (Abiola *et al.,* 2009). Before groundwater extraction, rigorous geophysical study is usually important to understand the subsurface lithology and aquiferous zones, such as fractures, faults, and joints, which are favorable to groundwater accumulation and groundwater quality.Inadequate data coverage might occasionally impede groundwater development and management through geophysical research and other traditional methods such as geostatistical and numerical modeling (Eyankware *et al*., 2022a). The evaluation of groundwater potential and aquifer vulnerability in typical complicated basement terrains has been the subject of much international research (Akintorinwa 2015; Joel *et al*., 2016; Akindeji 2020; Ayua *et al.,* 2024). These studies frequently assessed the potential of groundwater independently by analyzing hydrogeological and geoelectrical characteristics such transmissivity, hydraulic conductance, aquifer thickness, and resistivity. As evidenced by Eyankware, *et al*., (2022b), Umayah and Eyankware (2022), and Eyankware and Aleke (2021), the use of geophysics in the investigation of aquifer vulnerability has grown in popularity.Geophysical techniques, particularly electric resistivity approaches, can be used to estimate building foundations, groundwater distribution, and aquifer vulnerability, among other things. Geophysical instruments were used by Eyankware *et al*., (2022) and Eyankware and Aleke (2021) for groundwater exploration (Al-Garni *et al*., 2005; Eyankware and Umayah, 2022). Similar to this, a variety of geophysical techniques, such as ground-penetrating radar, seismic, electrical resistivity, and gravity, can be employed to look for groundwater resources (Kearey, *et al*., 2002). The electrical resistivity approach, which uses a Schlumberger electrode array and vertical electrical sounding, can be used to investigate the spatial distribution and depth of various hydro-lithostratigraphic units (Ebong *et al*., 2016; Akpan *et al.,* 2013, 2014). Ebong *et al*., (2016) and Igwe *et al*., (2022) claim that this approach is quick, inexpensive, non-invasive, and environmentally benign. It also needs equipment that is easily accessible. However, because there are intrinsic issues with how electrical resistivity data are translated to geology models, inaccuracies are occasionally discovered in this data (Ebong *et al*., 2014). Typically, the ambiguities are cleared out by integrating geophysical and geological data (Ebong *et al.,* 2016). Apart from the previously mentioned limitations, Kearey *et al*, (2002) state that the electrical resistivity approaches cannot be utilized to explore depths exceeding 1000 meters. However, previous studies conducted in this field have indicated that water-carrying units are located at a depth of less than 1000 meters (Abiola *et al.,* 2009; Olorunfemi and Fasuyi 1993). To the best of our knowledge, there has been no prior published research conducted on aquifer vulnerability and groundwater flow direction in the study area, making this investigation particularly significant. Evaluating the sensitivity of aquifers in this region is essential to ensure that the local population has continuous access to safe water for various uses, especially given that improper waste disposal evidenced by the prevalent open dumpsites in the area poses risks to both human health and aquatic ecosystems. The residents of Orire Estate in Akure, Ondo State, have reportedly faced challenges related to low groundwater potential and contamination, underscoring the need for this geophysical study. Therefore, the objective of this paper is to assessed the aquifer protective capacity of Orire Estate in Akure, Ondo State, Nigeria

MATERIALS AND METHOD

Location, Physiography, and Accessibility: The study area is located between latitudes 8° 16′ N and 8° 18′ N and longitudes 7° 31′ E and 7° 37′ E (see Fig. 1). The research area, Orire Estate, Akure, is situated in Nigeria's southwest region. mostly composed of gabbroic and diorite rocks; quartzite; meta-sedimentary rocks, meta-igneous rocks, charkockite,

gabbroic and granitic rocks; and the members of the earlier granite suite, which are primarily composed of granites, granodiates, and syenites, see Fig. 1 displays the research area's base map. The site is located on gently rolling ground and is surrounded by outcroppings of granitic rock. Between 303 and 335 meters is the range of elevation. While Oba-Ile Akure experiences year-round rains, the available rainfall data indicates that the heaviest rains occur in November and the heaviest rains occur in March. The north receives 1150 mm of rain annually, whereas the south receives 2000 mm. Rainfall decreases in both quantity and dispersion as one moves inland from the coast (Akinseye 2010; Akinseye *et al*. 2012). According to Ayolabi *et al*. (2003), the research area has bedrock ridges and depressions with structural fault zones that are viable for groundwater establishment. Adedipe *et al*., (2014) also carried out a geophysical investigation in the research region to evaluate its capacity to protect aquifers and its potential for groundwater. It was advised that the aquifer be secure and that a low-to medium-capacity borehole be dug in the research region. Eebo and Yusuf (2021) found that the study area is mostly composed of a medium aquifer, with relatively few areas being non-aquiferous.

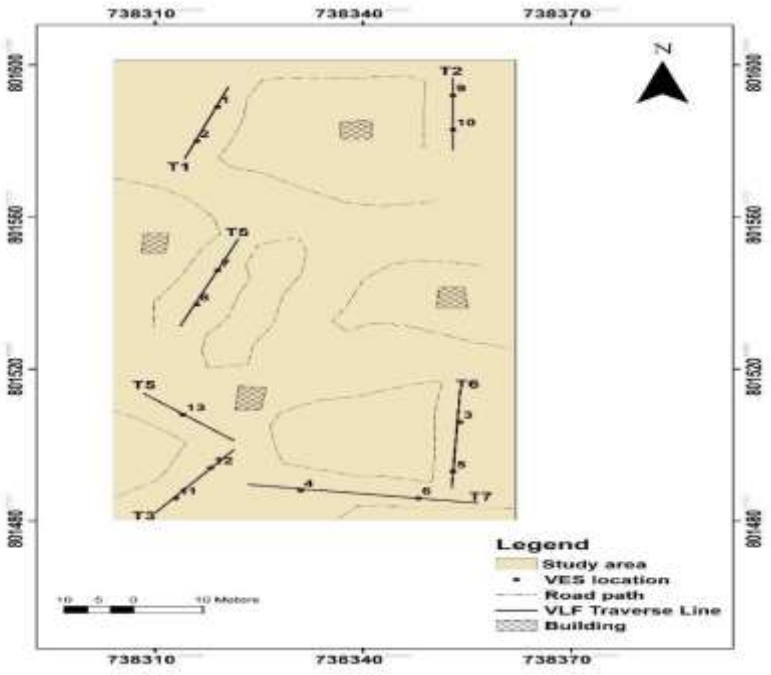

Fig.1: Base map of the study area.

Geology, and hydrogeology: The Precambrian Basement complex rocks of Southwestern Nigeria (Rahaman 1988) underlie the research region. These rocks are classified into two main petrologic units: migmatite gneiss and biotite-granite; refer to Fig. 2. There are granitic and biotite gneiss outcrops in the western portion of this study region. In a similar vein, the western street of the study area is home to granite boulders and charnokites. Surface layers with varying porosity and permeability are created by weathering processes and are present in typical basement topography in tropical and equatorial regions (Odunsanya and Amadi 1990). The fact that crystalline basement rock from the Precambrian age covers more than half of Nigeria limits the amount of groundwater available there (Kazeem 2007). This geological landscape is primarily composed of igneous and metamorphic rocks, such as granite gneisses and migmatites. In the north-central region of Kaduna State, Nigeria, DanHassan and Olorunfemi (1999) used the electrical resistivity method to identify various subsurface geoelectrical layers, aquifer units and their properties, the subsurface structure, and its impact on the overall hydrogeological condition. Finding water-bearing units in an area underlain by basement-complex rocks is generally a challenging task, according to earlier writers (Aboh and Osazuwa 2000; Olurunfemi and Fasuyi 1993). Due to the highly localized water-producing zones and the wide variation in lithology and structure, groundwater exploration is challenging (Abiola *et al*., 2009; Olurunfemi *et al*., 1999; Oladapo *et al.*, 2004). In basement complex sites, high topographical characteristics (ridges, for example) that are linked to high bedrock relief are among the factors that are looked at for a potential well site. In some regions, this

is an important issue for location. Wells located on fat terrain and valleys tend to yield more water than wells located on hilltops and valley sides because the crests of bedrock ridges, when present, act as a radiating center for groundwater as water normally drains along steep slopes and hilltops to a point of discharge in adjacent lowlands (Olorunfemi and Okhue 1992). In metamorphic terrains, well locations can be determined using fault breccias (Olorunfemi and Okhue 1992). Under ideal circumstances, groundwater flow is inhibited by features such as reefs that slice across short sections of valleys with high recharge areas, hornblende gneiss, and basic dykes (Akakuru *et al*., 2023). Nonetheless, worn rocks exhibit both fracture and intergranular porosities. Permeability is somewhat decreased by the clay content of the weathered section. A small hamlet or village can have access to enough water from weathered and fractured aquifers in hard rock locations (Patrick *et al*., 2021). Aquifers are created in crystalline rocks by weathered, partially weathered, or fractured zones (Olorunfemi and Okhue 1992). The presence of cracks at depth and advantageous morphological features at the surface are the primary factors that influence the kind and degree of weathering.

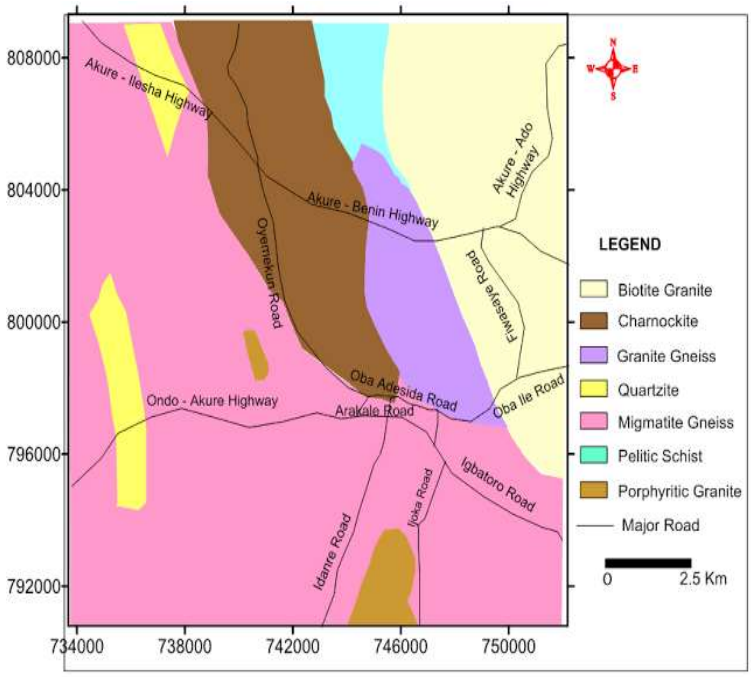

Fig. 2: Geology of the study area

Methodology: An OHMEGA Terrameter and its accessories were used to conduct thirteen (13) VES within the study region, as depicted in Fig. 1. With a maximum half current (AB/2) electrode separation of 100 m and a half potential (MN/2) electrode separation of 5 m, a Schlumberger electrode array was utilized for every VES profile. Spatial distribution maps of S, Tr, ρL, and ρt were created using Surfer program. The observed field data was converted to apparent resistivity (a) values using equation 1:

$$\pi\left(\frac{\left(\frac{AB}{2}\right)-\left(\frac{MN}{2}\right)}{MN}\right)\Delta V/I \qquad (1)$$

In order to develop field curves that were smoothed to remove small cusps caused by mistakes or local impacts, the apparent resistivity (ρa) data was plotted against the half current electrode spacing (AB/2) in a bi-logarithmic manner. This produced the geoelectric curves. In order to obtain start-up models that were inverted using WinRESIST software, these smoothed curves were compared with standard and auxiliary curves using the semi-quantitative auxiliary point method (Joshua *et al*., 2023; Ayua *et al*., 2024) in an iterative process to determine the one-dimensional geoelectric properties, including real layer resistivity and thickness, beneath the VES station. The root mean square (RMS) error was used to measure the modeling accuracy. Results with errors less than 5% were accepted, while models that had errors over this cutoff were refined until a good match was obtained.

The lithologies associated with the geoelectric section were interpreted through the use of standard charts that were supplied by Kearey, Brooks, and Hills (2002)

and Loke (1999). Several elements related to the combinations of thickness and resistivity of the geoelectric layers must be taken into account for a thorough study and comprehension of the geological model (Zohdy *et al*., 1974; Maillet, 1947). Among these are the transverse resistance (T) and longitudinal conductance (S), which are commonly referred to as Dar Zarrouk parameters.

Dar Zarrouk's longitudinal (S) and transverse (T) parameters were derived via

$$S = \frac{h}{p} \qquad (2)$$

$$T = hp \qquad (3)$$

Where h is the aquifer thickness and p is the aquifer resistivity

Longitudinal Unit Conductance (*S*) was calculated using equation 4 as proposed by Asfahani, (2013); Eyankware , (2019). The longitudinal conductance is equal to the number of layers (n).

$$S = \sum_{i=1}^{n} \frac{h_i}{\rho_i} = \frac{h_i}{\rho_i} + \frac{h_2}{\rho_2} + \cdots + \frac{h_n}{\rho_n} \qquad (4)$$

Transverse Resistivity was determined from equation 5 as proposed by Suneetha and Gupta (2018)

$$\rho_t = \frac{T}{H} = \frac{\sum_{i=1}^{n} h_i \rho_i}{\sum_{i=1}^{n} h_I} \qquad (5)$$

Groundwater Flow Direction: Using the groundwater modeling system software (GMS), which makes use of the study area's elevation and geographic coordinates as well as other pertinent data like the hydraulic conductivity of the geology formation present, well, river, recharge, lake, stream information, etc. if available, the groundwater flow direction of the study area was generated. The geo-electrical sections, which were created using the data from the sounding curves, were used to calculate the thickness of the aquifer.

Very Low Frequency Electromagnetic (VLF-EM) Survey: The (VLF-EM) technique utilizes radio signals in the 10–30 kHz frequency range to evaluate the electrical properties of near-surface soils and shallow bedrock (Ayobolu and Eyinla, 2022). This method allows for the rapid and cost-efficient acquisition of VLF profiles to detect anomalous conductive features. It finds extensive applications across various fields, including environmental studies, groundwater exploration, mining, and engineering surveys. Additionally, VLF can identify long conductors such as electric cables and pipelines, as well as electrically conductive structures like fault zones, which typically exhibit greater conductivity than the surrounding rock (Gnaneshwar *et al.,* 2011; Ayobolu and Eyinla, 2022). VLF receivers measure current density resulting from both primary and secondary magnetic fields, facilitating the identification of water-saturated fracture zones, mineralized areas, and metallic objects, which are critical for groundwater exploration and contamination evaluation (Gnaneshwar *et al.,* 2011).

Many filtering approaches are commonly utilized in the qualitative interpretation of VLF-EM data, with the Fraser and Karous–Hjelt methods being the most commonly used (Fraser, 1969; Karous and Hjelt, 1983; Ayobolu and Eyinla, 2022). In order to enhance the signal-to-noise ratio of the dataset and bolster the anomalous signature, the real (tilitangle) VLF-EM data and its imaginary component were subjected to Spitzer filtering with the use of KarousHjelt software. This helped with qualitative interpretation and improved the signals of conductive structures.

RESULT AND DISCUSSION

Within the research region, seven traverses in the directions of S-N, N-S, E-W, and W-E were established. The Very Low Frequency Electromagnetic Method and the Electrical Resistivity Method employed vertical electrical sounding (VES) as two geophysical approaches for this survey. The ABM WADI was used to carry out the VLF-EM measurements along the defined traverses. Each traverse had 30 stations built, spaced 5 meters apart from one another.

Fixed centroid resistivity measurements were used to measure vertical variation in the ground apparent resistivity during the geoelectric survey by gradually widening the distance between the electrodes about a fixed centre of array.

Tables 1 and 2 present an overview of the 13 VES curves generated across the studied area. Four underlying geometric layers were found for these components. These include the top soil, worn layer, cracked basement, and basement rock. The curve types are comprised of four (four) three-layer models (K, A, and H) and nine (9) four-layer earth models (KH, A, AA, HA, and KA), as Tables 1 and 2 demonstrate. Samples of the AA curve type are shown in Figs. 3 and 4, which show the results of the partial curve matching produced by the Winrest software. Tables 1 and b demonstrate that the A-type and A-type covered 38.5% of the research region, whereas the KH-type, HA, and HA-type covered 7.7%.

Table 1: Summary of interpreted VES (1-5) results obtained from the study area

VES Number	Curve Types	Number of layers	Resistivity (Ω-m)	Thickness (m)	Depth (m)	Probable Lithology
1	KH	1	133.0	1.0	1.0	Top Soil
		2	257.4	4.4	5.3	Weathered layer
		3	229.3	8.1	13.4	Fractured basement
		4	2776.8	----	-----	Fresh Basement
2	AA	1	91.0	1.2	1.2	Top Soil
		2	162.4	4.9	6.1	Weathered layer
		3	362.1	17.3	23.5	Fractured basement
		4	3117.4	------	------	Fresh Basement
3	AA	1	91.9	1.0	1.0	Top Soil
		2	386.5	10.0	10.9	Weathered Layer
		3	984.9	19.2	30.1	Partly Fractured Basement
		4	2305.1	------	------	Fresh Basement
4	AA	1	82.3	1.0	1.0	Top Soil
		2	722.9	3.1	4.1	Weathered Layer
		3	2513.0	10.1	14.4	Partially Fractured Basement
		4	5790.5	------	-----	Fresh Basement
5	A	1	56.3	1.3	1.3	Top soil
		2	125.6	7.8	9.1	Weathered layer
		3	358.6	----	-----	Fractured basement
6	A	1	160.0	1.0	1.0	Topsoil
		2	1192.1	12.8	13.9	Partly Fractured Basement
		3	5739.4	----	-----	Fresh Basement
7	HA	1	870	0.9	0.9	Top Soil
		2	90	2.6	3.6	Weathered layer
		3	872	20.5	24.0	Partly Fractured Basement
		4	1582.8	------	-----	Fresh Basement
8	AA	1	130.6	1.2	1.2	Top Soil
		2	296.1	6.2	7.5	Weathered layer
		3	1082.3	23.7	31.1	Partly Fractured Basement
		4	4219.3	-----	-----	Fresh Basement
9	AA	1	164.9	1.2	1.2	Top Soil
		2	286.5	6.6	7.8	Weathered layer
		3	311.1	17.8	25.6	Fractured basement
		4	1423.1	----	-----	Fresh Basement
10	AA	1	198.4	1.0	1.0	Top Soil
		2	978.7	13.6	14.6	Weathered layer
		3	3041.8	20.5	35.1	Partly Fractured Basement
		4	3783.6	-----	------	Fresh Basement
11	A	1	77.4	1.2	1.2	Top Soil
		2	250.2	12.3	13.4	Weathered Layer
		3	356.7	-----	-----	Partly Fractured Basement t
12	KA	1	138.9	1.0	1.0	Top Soil
		2	87.0	3.0	4.0	Weathered layer
		3	829.8	10.2	14.2	Partly Fractured Basement
		4	3561.1	------	----	Fresh Basement
13	A	1	57.0	1.5	1.5	Top Soil
		2	159.3	17.1	18.7	Weathered Layer
		3	896.4	-----	-----	Partly Fractured Basement

Table 3: Summary of the second order parameters derived from the study area

VES	Easting	Northing	Longitudinal Conductance	Overburden Thickness	Traverse Resistivity	Hydraulic Conductivity
1	738319	801589	0.024639	5.4	133	0.010345
2	738316	801580	0.043434	6.1	91	0.00397
3	738354	801506	0.036709	11	92	4.47E-05
4	738331	801488	0.016483	4.1	82	7.46E-10
5	738353	801493	0.023214	1.3	56	0.021717
6	738348	801486	0.00625	1	160	1.01E-05
7	738319	801546	0.029923	3.5	870	0.000101
8	738316	801537	0.030106	7.4	131	2.23E-05
9	738353	801592	0.030269	7.8	165	0.005732
10	738353	801583	0.018942	14.6	198	1.65E-11
11	738313	801486	0.015584	1.2	77	0.008893
12	738318	801494	0.041677	4	139	0.000137
13	738314	801508	0.026316	1.5	57	0.017124

According to Akinlalu *et al*. (2017) and Joshua *et al*., (2023), the studied area shows substantial variability in resistivity sounding curves, which is indicative of heterogeneity typical of a multipart geologic setting. The curves in Figs. 3 and 4 demonstrate the high degree of precision of the field data since their root mean square (RMS) error is sub-unity, which is less than the 5% threshold values used by other studies, as reported by Joshua *et al*., 2023.

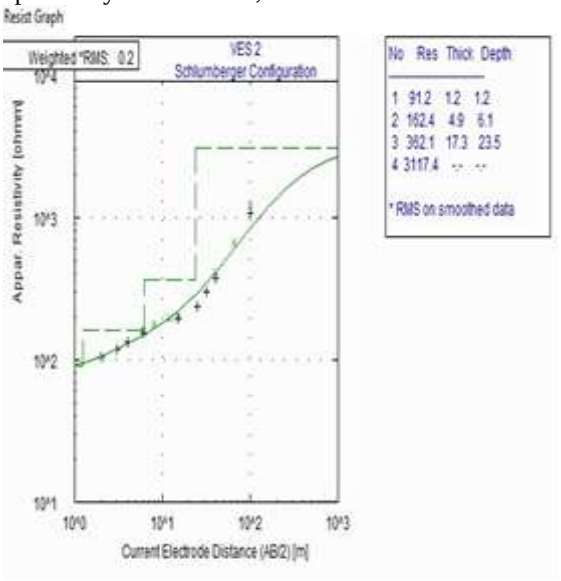

Fig.3: VES 2 curve matching result

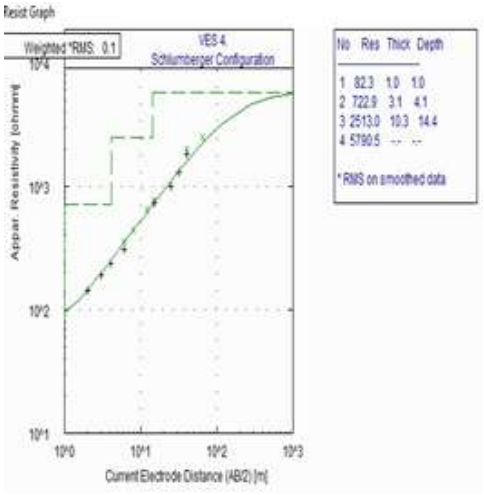

Fig.4: VES 4 curve matching result

The topsoil is the first stratum. Along these profiles, the thickness of the topsoil is rather thin, ranging from 0.9 to 1.5 m, whereas the resistivity value ranges from 57.0 to 198.4 Ω-m. Laterite, clay, sandy clay, and clayey sand make up the topsoil. The weathered layer is the second layer, the weathered layer's thickness varies from 2.6 to 17 in all the profiles. Moreover, the resistivity values span from 87.0 to 978.7 Ω-m. The partially broken and fractured basement makes up the third stratum. This layer's thickness varies from 7.8 to 23.7 m, while its resistivity values range from 311 to 3041.8 Ω-m. The fourth layer is the fresh basement, which has resistivity values ranging from 1423.1-2790.5790.57Ω-m. The thickness and depth of the final layer in the geo-electrical analysis are infinite (Obiabunmo *et al.,* 2014). In basement areas where groundwater accumulation is influenced by the thickness of the weathered layer and fractured bedrock, the thickness of this layer is essential for classifying the vertical extent of different geological types in the subsurface (Patra and Nath, 1999). In crystalline environments, a thicker overburden increases the potential for successful groundwater exploration. Furthermore, fractured bedrock has been identified as a particularly promising factor for groundwater exploration in crystalline terrains (Anomohanran*et et al.,* 2017; Falebita and Ayua, 2023).

Geo-electric Sections

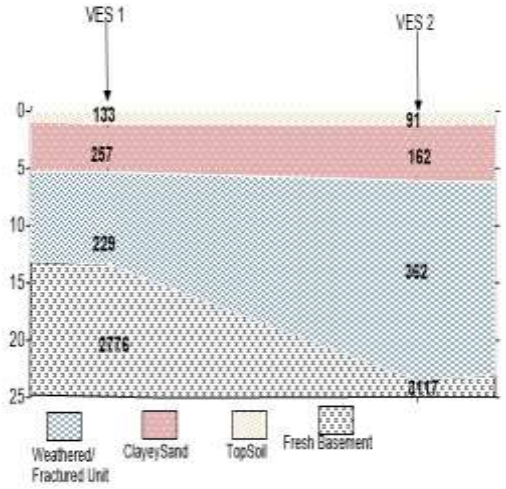

Fig. 5: Geo-electric section ofTraverse1 b

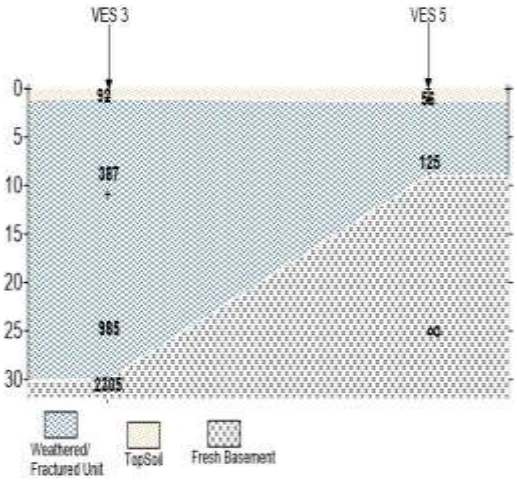

Fig. 6: Geo-electric section of Traverse 2

Fig. 5 to 9 illustrate the five geo-electric sections generated during the investigation based on the geo-electrical parameters obtained along the traverses. This illustration aims to depict the vertical and horizontal distribution of apparent resistivity (ρa) in the subsurface (Adagunodo, 2013). It highlights the relationship between vertical and horizontal facies changes inferred from the geo-electrical parameters (Adagunodo *et al.,* 2013a, b). Within these sections, four subsurface geo-electric strata were identified: the basement rock, the weathered layer, the topsoil, and the fractured basement. The top soil is the first stratum. Along these profiles, the thickness of the topsoil is rather thin, ranging from 0.9 to 1.5 m, while the resistivity value ranges from 57.1 to 198.4 Ω-m. The components of the topsoil are laterite, clay, sandy clay, and clayey sand. It is the weathered layer, the second layer.

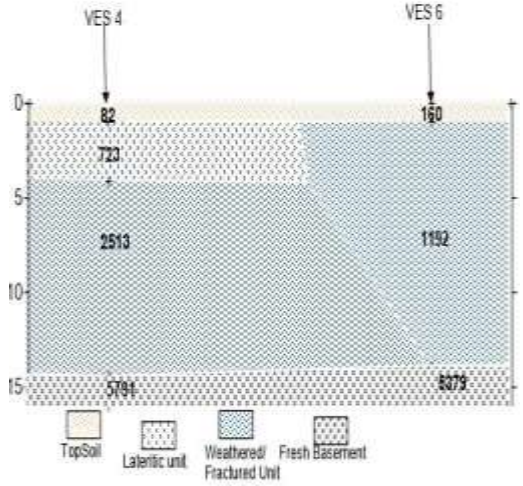

Fig. 7: Geo-electric section of Traverse 3

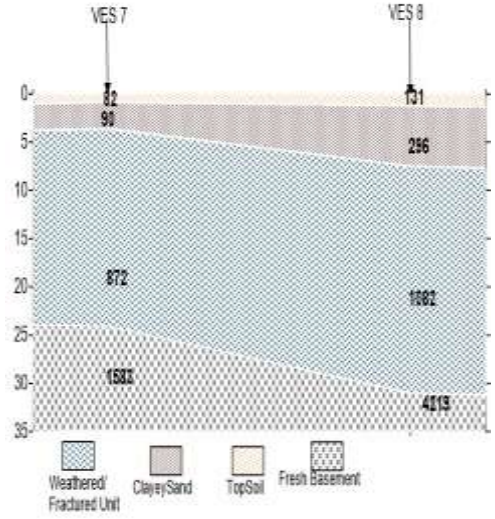

Fig.8: Geo-electric section of Traverse 4

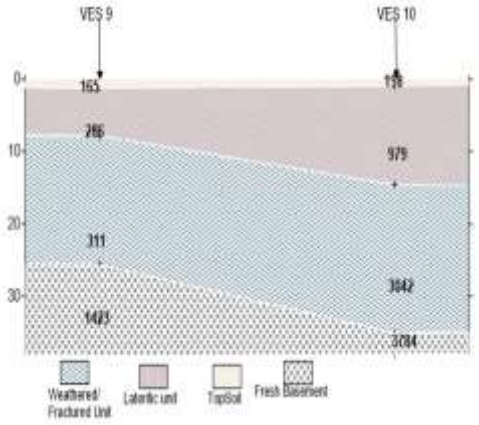

Fig. 9: Geo-electric section of Traverse 5

The range of profiles for the thickness of the weathered layer is 2.6–17 m. There is also a range of resistivity values from 87.0 to 978.7 °C. Both the partially fractured and fragmented basements make up the third stratum. While the resistivity values range from 311 to 3041.8 m, the layer's thickness ranges from 7.8 to 23.7 m. It is the fresh basement, the fourth layer. The resistivity values of this material range from 1423.1 to 2790.57 m. The worn layer and top soil are indicated by relatively low resistivity values of less than 100 Ω, which may indicate the presence of conductive materials, such as fluids or leachates from the wasted uppermost layer of soil.

VLF-EM: We used the Karous–Hjelt filters to evaluate the field-collected VLF-EM data qualitatively. It is evident from the filtered data and the relative current density pseudosections that were produced that the region has a variety of shallow and deep conductive zones. Fig. 10–13show the EM profiles that were produced and established in well-defined orientations to cover the research region. The VLF-EM traverses of the research area were undertaken in three directions: east-west, west-east, and south-north directions. The pseudosections of the VLF-EM data in Fig. 10-13 show contours of high and low conductive zones. Zones with red colour contours are intervals with high conductivity. Traverse 1 (Fig. 10) reveals low-conductivity zones, notably featuring a slightly reduced conductivity region between 80 and 105 meters, which is intersected by a conductive zone indicated by a reddish point on the 2-D image at approximately 85 to 90 meters corresponding to the high peak. The high peak of conductivity observed may be deduced to have been caused by faults or fracture zones with conductive fluids. Additionally, there are noticeable drops in conductivity at distances of 30 to 35 meters, 70 to 75 meters, and 110 to 120 meters, as highlighted by the yellow colour codes on the Fig. Traverse 2 (Fig. 11) also highlights low

conductivity regions indicating areas of poorly conducting materials. It depicts the locations of weakly conducting zones (greenish areas on the 2-D image) between 60 and 100 meters. At the beginning and end of the traverse, there are sections of low conductivity zones of 3-40 m and 100-120 m, respectively (orange colour codes on the 2-D image). Traverse 3 (Fig. 12) depicts the line of low conductivity with conductivitity gradually increasing from left to right along the traverse. Low conductivity locations ranging from 40 to 90 meters are identified at the start of the traverse (yellow points on the 2-D image). At a distance of 90-200 m, the traverse shows another site of medium conductivity (green spots on the 2-D image), slightly increasing towards the end of the traverse. Generally, there is largely homogenous line of low conductivity, possibly signifying intervals with partially weathered zones containing some amount of water or clayey layers which could act as a protective seal for aquifers in this area. Fig. 13 depicts the low conductivity area in Traverse 4. At a distance of 85–90 meters, a region of relatively high conductivity (represented by the yellow point on the 2-D image) is shown splitting into an area of floral conductivity (represented by the green point). The high peak of conductivity observed may be deduced to have been caused by faults or fracture zones with conductive fluids. Additionally, a zone of negative conductivity, marked by blue colour on the contour map, intrudes upon another flow conductivity area at a distance of 60 to 65 meters. Overall, these traverses provide critical insights into the conductivity patterns present in the study area, facilitating a better understanding of the subsurface geoelectric characteristics.

VLF-EM Profile: The VLF-EM sections are presented in figures 10a to 13b.

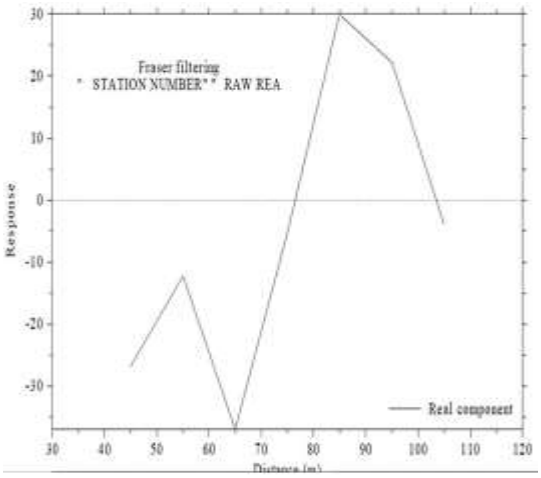

Fig. 10a: Response against distance of VLF EM profile along traverse1

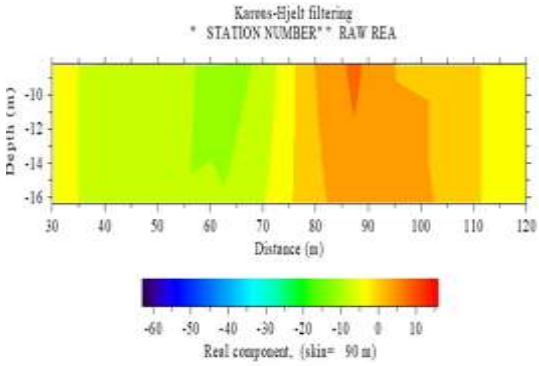

Fig. 10b: VLF-EM 2D-profilegenerated along traverse1

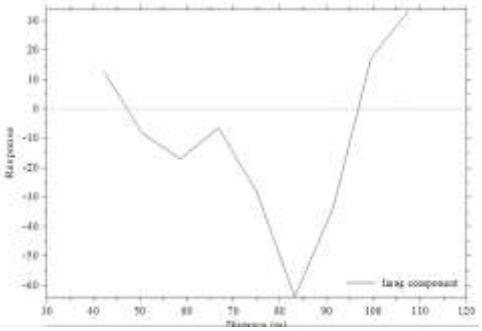

Fig. 11a: Response against distance of VLF EM profile along traverse 2

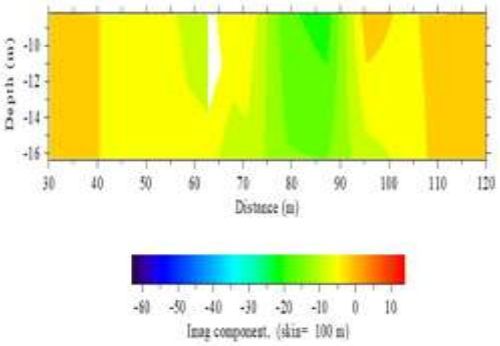

Fig. 11b: VLF-EM 2-D ProfileGenerated along Traverse 2

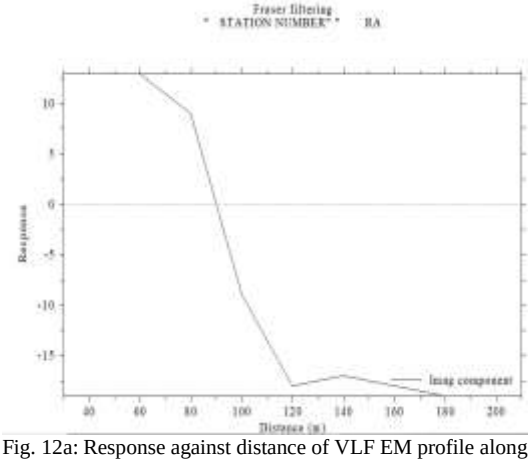

Fig. 12a: Response against distance of VLF EM profile along traverse 3

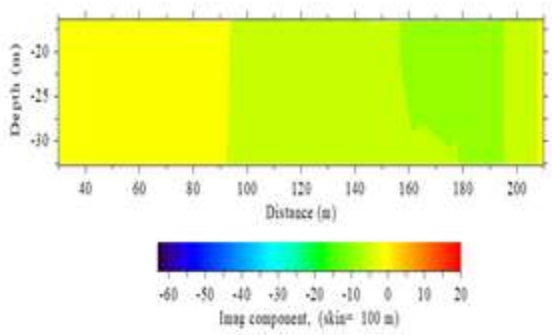

Fig.12b: VLF-EM 2-D Profilegenerated along Traverse 3

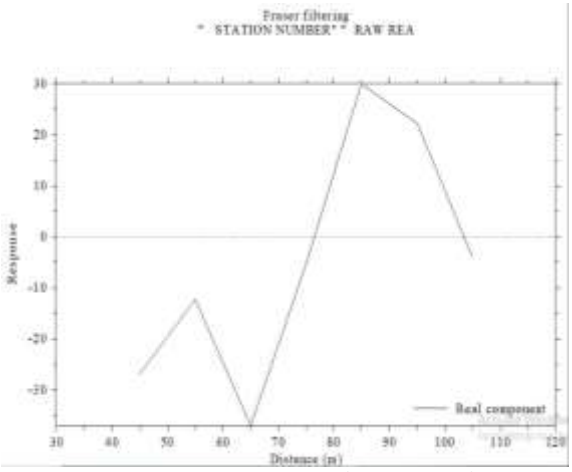

Fig. 13a: Response against distance of VLF EM profile along traverse 4

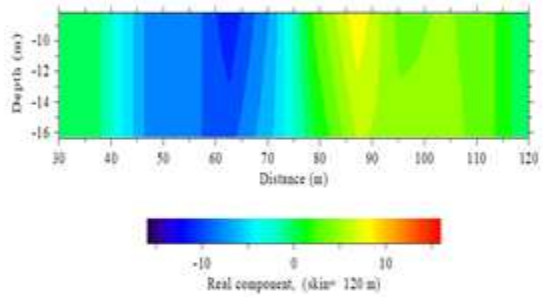

Fig. 13b: VLF-EM 2-D Profilegenerated along Traverse 4

Evaluation of Aquifer Protective Capacity: According to Oni *et al*., (2017), longitudinal conductance can be used to determine the level of groundwater protection against contaminants' vertical infiltration. It is the conductance through a 1 m column in the direction of the bedding plane. S is used to represent it (Nwanko *et al*. 2011). Table 4 displays the research area's overburden protective capacity. The primary impediment to the contamination of aquifers is the presence of overlying strata, whose restricted permeability regulates the delay between the infiltration of contaminants and their subsequent movement into the aquifer. As noted by Ayua *et al* (2024), the longitudinal conductance (S) of the overburden materials is directly correlated with the protective capacity of the overburden as it is as an indicator of the clay (a highly impervious geomaterial) content present. This means that the comparatively high longitudinal conductivity serves to safeguard the underlying aquifer. Aquifer in the research area is susceptible to surface pollution, as demonstrated by the values of longitudinal unit conductance (S) that were measured there and range from 0.0063 to 0.044 mhos. According to earlier research by Akinseye *et al.*, (2023), this is consistent. The longitudinal unit conductance values from the research region confirm that the overburden materials in the area are not able to adequately protect the aquifer, according to the classification shown in Table 4 by Oladapo *et al.*,. (2004).

Table 4: Aquifer protective capacity rating.

Longitudinal Conductance (mhos)	Aquifer Protective Capacity rating	VES Points
>10	Excellent	
5-10	Very good	
0.7-4.49	Good	
0.2-0.69	Moderate	
0.1–0.19	Weak	
<0.1	Poor	VES 1

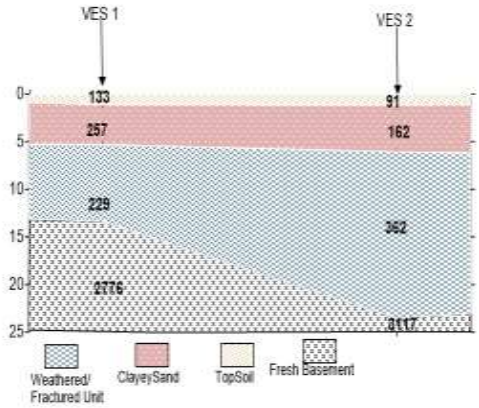

Fig. 14: Geo-electric section of traverse1.

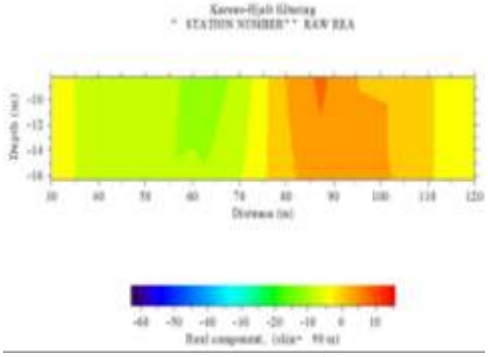

Fig. 15: b2- DVLF image ofTraverse1

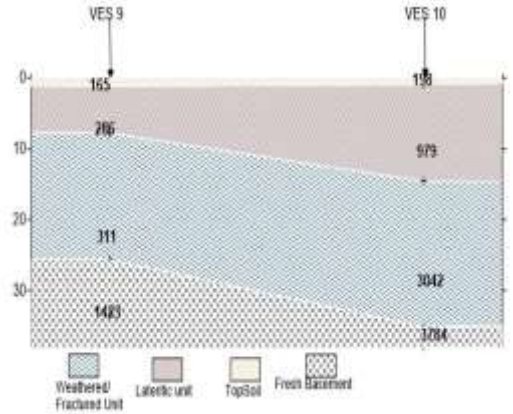

Fig. 16: Geo-electric section for Traverse 2.

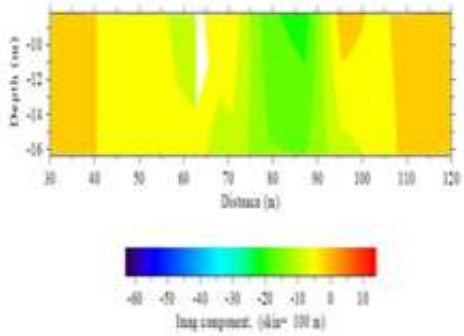

Fig. 17: 2-DVLF image of Traverse 2

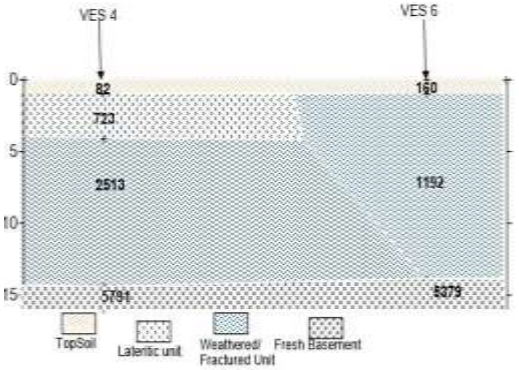

Fig. 18: 4.8.aGeoelectric section of Traverse 3.

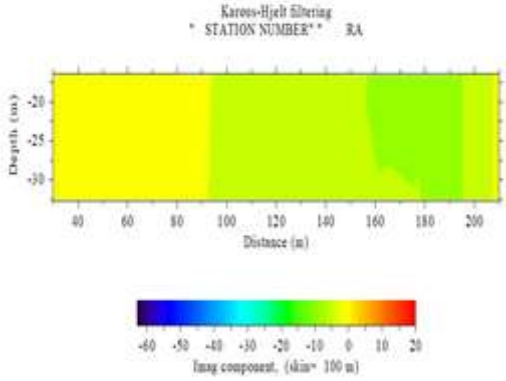

Fig.19:2-DVLF image of Traverse 3a)

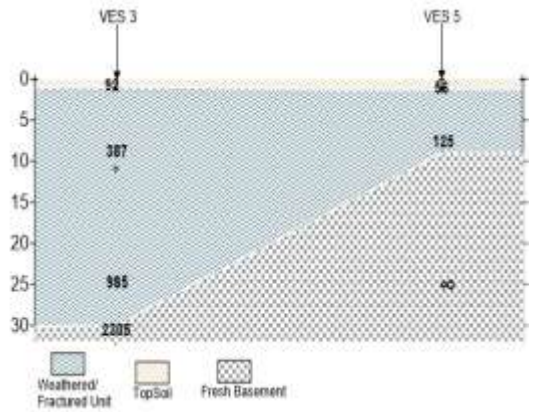

Fig.20: Geo-electric section of Traverse 4

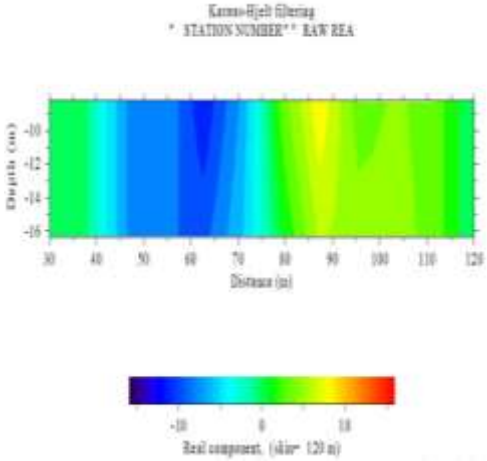

Fig.21:2-D VLF image of Traverse 4

Discussion on Correlated VLF-EM and VES: Figs. 5 to 9 depict the association between the geoelectric section and VLF-EM profiles of the five traverses. The topsoil has a relatively shallow thickness of 1.0 to 1.2 m, as seen in Fig. 14. The four layers are fresh basement, fractured layer, clayey sand layer, and top soil. Exceeding 2,500 m is the resistivity range of the newly formed basement. Low conductivities between 25 and 70 meters and an increase in conductivity between 75 and 80 m are shown in the VLF-EM image (Fig. 12). The traverse's 75–80 m conductivity spike cannot be interpreted as the presence of a geological structure since the change in conductivity value was too small. Fig. 16 shows that the topsoil of both VES stations in this traverse has a relatively thin thickness, with resistivity above 160 °C, ranging from 1.0 m to 1.2 m. The geo section reveals that the traverse is made up of four layers: fresh basement, feathered layer/partially fractured layer, lateritic unit, and topsoil. The resistivity of the fresh basement is more than 1400 m. The VLF-EM imagine (Fig. 17) shows extremely low conductivities over its whole length. The values of the high resistivity and low conductivities suggest that they are not linear

structures, such as faults or fractures. Fig. 20 includes VES 3 and VES 5. There are three layers: fresh basement, fractured unit, and topsoil. The range of soil thickness is 1.0–1.3 m. The thickness of the weathered layer varies from 25 to 29 meters at VES 3. The VLF-EM image (Fig. 21) shows that conductivity is very low at the beginning of its passage (30–37 m), then very low between 45 and 65 m. Between 85 and 92 meters, the conductivity increases and then levels off toward the end of the traverse. It is not very likely to deduce the presence of a geological feature from the conductivity of the peak.

Overburden Thickness: Surfer software was used to contour the thick layer of overburden covering the bedrock at Orire Estate see Fig. 22 The aquifer geometry of the subsurface is shown by creating an overburden thickness map. The aquifer geometry of the subsurface is shown by creating an overburden thickness map. The topsoil and weathered zone are encased in the overburden. The map Fig. 22 showed that the research area's two locations—VES station 10 in traverse two (2) in the northeastern section and VES station 3 in traverse six (6) in the southeast—have thick overburden layers.

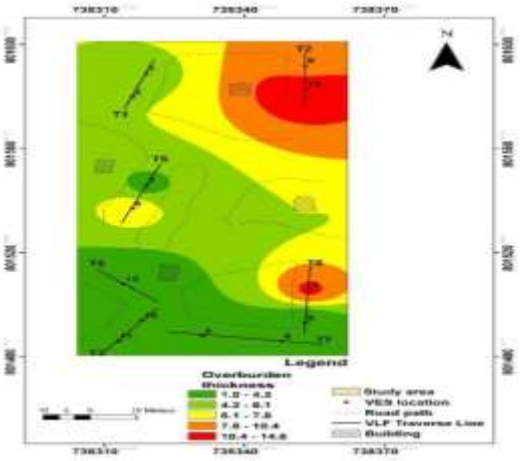

Fig. 22: Overburden Map of the study area.

The above-mentioned traverses range in thickness from 10.4 to 14.6 m. Fig. 22 overburden thickness map shows that VES station nine (9) in traverse 2 has a reasonably high thickness range from 7.8 to 10.4 m. Less than 10.4 meters is the thickness of the remaining investigation area. As noted by Sunmonu *et al.* (2012), "zones of high potential for groundwater exploration, especially in the Precambrian basement terrain, have been identified as areas with thick overburden equivalent to basement depression." The study area's northeastern overburden is extremely thick, and the southeasterly overburden has a likely significant groundwater potential. The less susceptible it is to superficial contamination, according to Danizman *et al*., (2017), the thicker the overburden layer. VES stations 2, 3, and 9 are thought to be less susceptible to contaminant intrusion.

Top Soil Resistivity: Fig. 23 showed the topsoil resistivity map. The research area's western portion, where VES stations 7 and 8 are located, has resistivity ranging from 566 to 870 m, top soil resistivity of 870 Ωm, VES station 7 has the highest, indicating that lateritic material covers the area. Fig. 22 illustrates that the very low to low classes occupy nearly 50% of the study area, indicating strong protection from the player. High clay content in this area is the reason for this. But there is little defense against the player in the other areas. Leachate or conductive fluids infiltrating into the subsurface from the above contaminants may be indicated by the very low resistivity areas surrounding VES stations 2, 3, 5, 11, and 13 (Fig. 23).

Iso-resistivity of weathered layer: The research area's aquifer is the weathered/fractured basement layer because of its capacity to hold and release a significant amount of groundwater. As can be observed in Fig. 24, the resistivity value of the aquifer is relatively high, ranging from 229 m to 1700 m. The lowest aquifer resistivity shown on the iso-resistivity map is 500 m, and it is located in the map's southernmost section. Low resistivity layers are used in groundwater housing, fault, and other linear structures. Both the northern-eastern and the southern-eastern regions of the chart display the maximum resistivity value of 1700°C.High resistivity areas won't make suitable aquifers. Transmissivity will be reduced. The aquiferous zone has high values in the studied area. It can be deduced that the location is not ideal for groundwater infiltration.

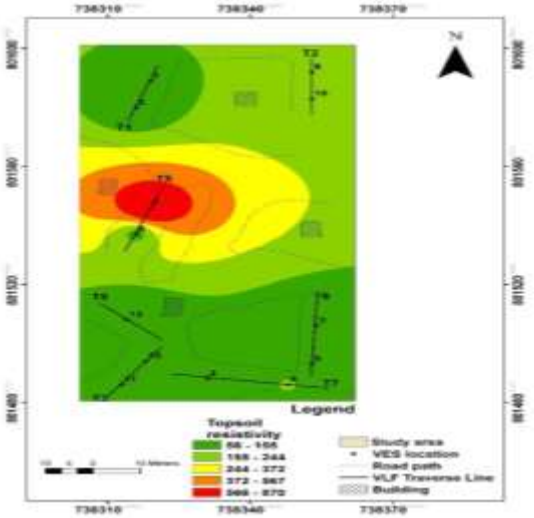

Fig. 23: Topsoil resistivity of the study area

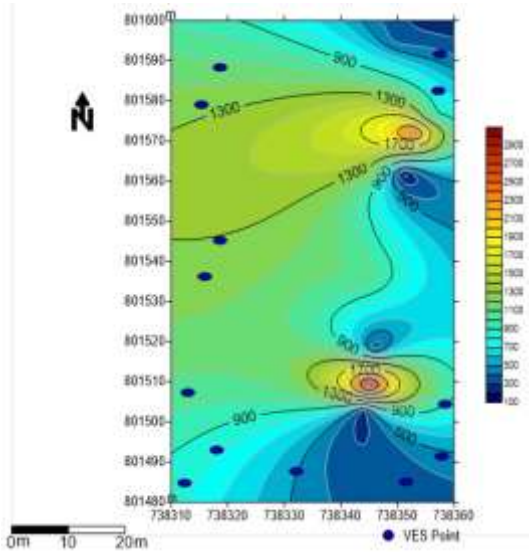

Fig. 24: Iso-resistivity map of weathered layer.

Longitudinal Conductance: Table 3 above indicates that the aquifer capacity rating in Table 3 gives the study region a negative grade and that its total longitudinal conductance is low, ranging from 0.00625 mhos (VES6) to 0.044 mhos (VES2). This suggests that the aquifer's ability to protect the area is limited. Figure 25 displays the longitudinal conductance map of the research region. The area is composed of areas with low to extremely low total longitudinal conductance. The western portion of the research area is dominated by the low total longitudinal conductance unit of 0.029 mhos to 0.044 mhos, which crosses VES stations 1 (VES stations 7 and 8) and 5 (VES station 1). The low total longitudinal conductance unit traverses 3 (VES station 2), 6 (VES station 3) and 2 (VES station 9) in the southern, southern-eastern, and northern regions, respectively. Located near the center of the research region is the moderately low total longitudinal conductance unit of 0.0248 mhos to 0.029 mhos. It extends to the northeast and reaches the southwest of the traverse region. It passes via 1 (VES stations 1) and 5 (VES stations 13). The extremely low total longitudinal conductance unit, which spans the southern and a tiny section of the northeastern regions of the research area, is between 0.0083 and 0.0248 mhos. This covers traverses 1, 7, 6, 5, and 2 (VES stations 10) as well as traverses 1 (VES station 1). This region's aquifer is highly vulnerable to pollutant penetration.

Hydraulic conductivity: Hydraulic conductivity, according to Eyankware and Umuyah (2022), is the physical ability of an aquifer to move water through pore spaces and fractures when exposed to a hydraulic gradient. This implies a negative proportionality to groundwater vulnerability. According to Table 3, the research area's hydraulic conductivity, K, ranges between 0 and 0.0123 m^2/day. Fig. 26 confirms that the region with high hydraulic conductivity corresponds to the area with low groundwater vulnerability.

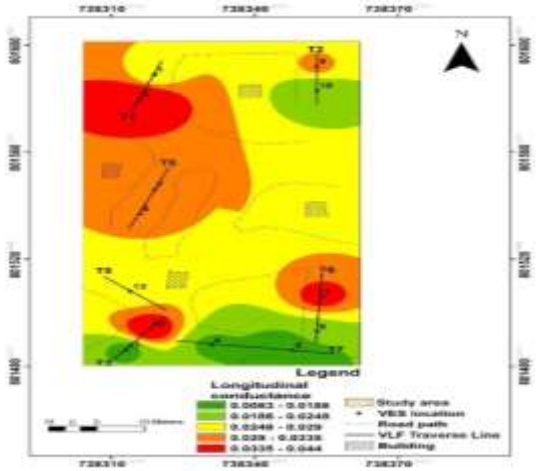

Fig. 25: Longitudinal conductance map of the study area.

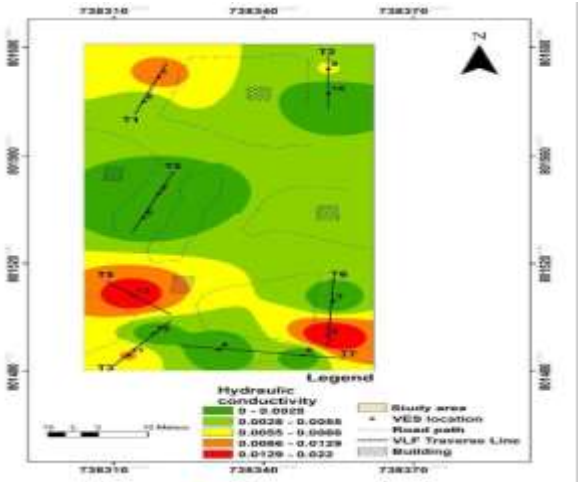

Fig. 26: Hydraulic conductivity map of study area.

Conclusion: Aquifer vulnerability in Orire Estate in Akure, Ondo State, Nigeria, has been determined by an integrated geophysical study that includes reconnaissance, electrical resistivity, and very low frequency (VLF) electromagnetic technique. Fourteen (13) and Four (4) were established. VLF-EM was used to map the conductive zones around the VES locations. The electrical resistivity (VES) result identified four subsurface layers: topsoil, weathered layer, fractured layers/partially cracked layers, and basement. The subsurface's aquifer protection rating is based on longitudinal conductance and can be categorized as excellent, very good, good, moderate,

weak, or bad. The characteristics of the overburden units' ability to protect the aquifer included their associated resistivity values and layer thickness. A unique and poor-quality zone for aquifer protection was delineated.

Declaration of Conflict of Interest: The authors declare no conflict of interest

Data Availability Statement: Data are available upon request from the corresponding author

REFERENCES

Akinlalu, AA; Adegburuyiro, A.; Adiat, KAN; Akeredolu, BE; Lateef, WY (2017). Application of multi-criteria decision analysis in prediction of groundwater resources potential: A case study of Oke-Ana, Ilesa Area southwestern, Nigeria. *J. Astron. Geophy*. 6(2017), 184–200.

Akinseye, VO; ·Osisanya, WO; Eyankware, MO; Korode, I.A; Ibitoye, AT (2023). Application of second-order geoelectric indices in determination of groundwater vulnerability in hard rock terrain in SW. Nigeria. *Sustainable Wat. Resour. Manage*. 9: 169, https://doi.org/10.1007/s40899-023-00936-w

Ayobolu, TO; Eyinla, DS (2020). Investigation of the Source of Groundwater Contamination Near a Farmland Using the VLF-EM and Magnetic Methods. *J. Environ. Earth Sci.* 12 (6): 39-52.

Ayua, K.J; Ilozobhie, AJ; Eju, DI; Agbasi, OE (2023). Scrutinate proclivity of regional aquifer hydraulic parameters: Apriorisms for borehole failures within parts of the middle Benue Trough, Nigeria. *Water Practice Tech*. 18(12), 3347–3364

Ayua, KJ; Alimi, GI; Bamigbaiye, FF; Arya, JA (2024). Synthesizing vulnerability indices within a diverse lithological context: Corollaries for groundwater quality assurance and surface layer corrosiveness of Lokoja Geomaterials, Nigeria. *Water Practice and Tech.* 00 0, 1

Eyankware, MO (2019). Integrated Landsat Imagery and Resistivity Methods in Evaluation of Groundwater Potential of Fractured Shale at Ejekwe Area, Southeastern Nigeria, Unpublished PhD Thesis

Eyankware, MO; Akakuru, OC; Osisanya, WO; Umayah, SO; Ukor, KP (2023) Assessment of heavy metal pollution on groundwater quality in the Niger Delta Region of Nigeria. *Sustainable Wat Resources Manage*. 9:189.

Eyankware, MO; Akakuru, CO; Eyankware, EO (2022a). Hydrogeophysical delineation of aquifer vulnerability in parts of Nkalagu areas of Abakaliki, SE. Nigeria. *Sustainable Wat. Resources Manage.* 8: 21-39

Eyankware, MO; Akakuru, CO; Ulakpa, ROE; Eyankware, EO (2022b). Hydrogeochemical approach in the assessment of coastal aquifer for domestic, industrial, and agricultural utilities in Port Harcourt urban, southern Nigeria. *Intern. J. Energy. Wat. Resour. 6: 1-20.*

Eyankware, MO; Aleke, G (2021). Geoelectric investigation to determine fracture zones and aquifer vulnerability in southern Benue Trough southeastern Nigeria. *Arab J Geosci*. 14: 1-22 https://doi.org/10.1007/s12517-021-08542-w

Falebita, DE; Ayua, K.J (2023). Appraisal of lineaments for groundwater prognosis in the Middle Benue Trough, Nigeria: a case study. *Sustain. Water Resour. Manag.9*, 12 https://doi.org/10.1007/s40899-022-00791-1

Fraser, DC. (1969). Contouring of VLF-EM data. *Geophy*. 34: 958 967

Gnaneshwar, P; Shivaji, A.; Srinivas, Y; Jettaiah, P; Sundararajan, N (2011).Very-low-frequency electromagnetic (VLF-EM) measurements in the Schirmacheroasen area, East Antarctica. *Polar Sci.* 5(1), 11–19.

Igwe, EO; Ede, CO; *Eyankware, MO;* Nwachukwu, CM; Onyekachi, BW (2022). Assessment of Potentially Toxic Metals from Mine Tailings and Waste Rocks Around Mining Areas of Oshiri-Ishiagu Region, Southeastern Nigeria. *Earth. Syst. Environ.* 5, 1-20

Karous, M; Hjelt, SE (1983). Linear filtering of VLF dip-angle measurements. *Geophys. Prospecting J., 31*, 782–794. https://doi.org/10.11648/j.ijrs

Opara, AI; Edward, OO; Eyankware, MO; Akakuru, OC; Oli, IC; Udeh, HM (2022). Use of geo-electric data in the determination of groundwater potentials and vulnerability mapping in the southern Benue Trough Nigeria. *Intern. J. Environ. Sci. Tech. 3 1-25*

Umayah, OS; Eyankware, MO (2022). Aquifer evaluation in southern parts of Nigeria fromgeo-electrical derived parameters. *World News. Nat. Sci.* 42; 28-43